

# UC Berkeley

## UC Berkeley Previously Published Works

### Title

A Ratiometric Sensor Using Single Chirality Near-Infrared Fluorescent Carbon Nanotubes: Application to In Vivo Monitoring

### Permalink

<https://escholarship.org/uc/item/5hp1c44g>

### Journal

Small, 11(32)

### ISSN

1613-6810

### Authors

Giraldo, Juan P  
Landry, Markita P  
Kwak, Seon-Yeong  
et al.

### Publication Date

2015-08-01

### DOI

10.1002/smll.201403276

Peer reviewed

# A Ratiometric Sensor Using Single Chirality Near-Infrared Fluorescent Carbon Nanotubes: Application to In Vivo Monitoring

Juan P. Giraldo, Markita P. Landry, Seon-Yeong Kwak, Rishabh M. Jain, Min Hao Wong, Nicole M. Iverson, Micha Ben-Naim, and Michael S. Strano\*

**A**dvances in the separation and functionalization of single walled carbon nanotubes (SWCNT) by their electronic type have enabled the development of ratiometric fluorescent SWCNT sensors for the first time. Herein, single chirality SWCNT are independently functionalized to recognize either nitric oxide (NO), hydrogen peroxide ( $H_2O_2$ ), or no analyte (remaining invariant) to create optical sensor responses from the ratio of distinct emission peaks. This ratiometric approach provides a measure of analyte concentration, invariant to the absolute intensity emitted from the sensors and hence, more stable to external noise and detection geometry. Two distinct ratiometric sensors are demonstrated: one version for  $H_2O_2$ , the other for NO, each using 7,6 emission, and each containing an invariant 6,5 emission wavelength. To functionalize these sensors from SWCNT isolated from the gel separation technique, a method for rapid and efficient coating exchange of single chirality sodium dodecyl sulfate-SWCNT is introduced. As a proof of concept, spatial and temporal patterns of the ratio sensor response to  $H_2O_2$  and, separately, NO, are monitored in leaves of living plants in real time. This ratiometric optical sensing platform can enable the detection of trace analytes in complex environments such as strongly scattering media and biological tissues.

## 1. Introduction

Single walled carbon nanotubes (SWCNT) are nanomaterials with extraordinary mechanical and electrical properties that have applications to the fields of electronics,<sup>[1]</sup> materials,<sup>[2]</sup> and sensors.<sup>[3,4]</sup> In particular, optical nanosensors have enabled the detection of analytes with high spatio-temporal

resolution.<sup>[5,6]</sup> Semiconducting SWCNT are excellent signal transducers for nanosensors due to their fluorescence stability, lifetime, and emission in the near-infrared (NIR).<sup>[7]</sup> Consequently, there has been much interest in developing nanosensors by noncovalent complexation of various wrappings with SWCNT, such that the SWCNT corona can recognize an analyte.<sup>[8]</sup> However, one challenge in using chemically responsive fluorescent probes is obtaining an absolute signal such that probe intensity can be used to calculate local presence of an analyte. In analytical chemistry, such probes are often employed as ratiometric sensors in which one of two distinct fluorophores report an analyte-independent reference signal to which the sensing signal is scaled.<sup>[9]</sup> To date, it has not been possible to generate a ratiometric sensor using carbon nanotubes because of difficulty in separating the nanotubes as distinct chiral species with characteristic emission wavelengths. In this work, we capitalize on recent

Dr. J. P. Giraldo, Dr. M. P. Landry, Dr. S.-Y. Kwak,  
R. M. Jain, M. H. Wong, Dr. N. M. Iverson,  
M. Ben-Naim, Prof. M. S. Strano  
Department of Chemical Engineering  
Massachusetts Institute of Technology  
Cambridge, MA 02139, USA  
E-mail: strano@mit.edu



DOI: 10.1002/sml.201403276

progress from our group and others in the separating and sorting of SWCNT<sup>[10–15]</sup> to generate the first SWCNT ratiometric fluorescent sensors.

In previous work, the signal observed from optical nanosensors was largely limited to the fluorescence response of a multichirality SWCNT sample with multiple peaks of NIR emission.<sup>[8,16–19]</sup> Other studies have also produced multimodal sensors, in which the same SWCNT wrapping generates distinct optical signals from different molecular interactions.<sup>[20]</sup> However, there are numerous advantages in developing SWCNT ratiometric sensors, particularly for analyte quantification in living systems,<sup>[17]</sup> where interfering biomolecules are abundant. Though a sensor may respond clearly to an analyte *in vitro*, it is often very difficult to limit the sensor response to the analyte of interest when the sensor is immersed into a complex and dynamic biological sample. One approach to optimizing sensor development relies on extensive screening of the sensor in the presence of possible interfering molecules.<sup>[8,18]</sup> This approach is time intensive and is therefore a significant limitation in the development of optical sensors. The signal from a nonresponsive reference chirality within a ratiometric sensor increases the certainty with which we attribute the observed response to the analyte presence, and can greatly facilitate and expedite future development of selective optical sensors. Additionally, single chirality SWCNT are brighter than multichirality SWCNT mixtures, reaching six times higher fluorescence on a per-mass basis.<sup>[21]</sup>

Despite the strong interest in the development of ratiometric optical sensors, several limitations have restricted their successful production from chirality-separated SWCNT. A main problem has been the relative difficulty in obtaining preparative-scale quantities of single-chirality SWCNT.<sup>[13]</sup> A common method for the production of single chirality SWCNT suspended in sodium dodecyl sulfate (SDS) relies on—preparative-scale separation through columns of Sephacryl<sup>[13,14]</sup> followed by coating exchange of SDS with other species by dialysis,<sup>[21]</sup> a time and labor-intensive process. Manual separation of large volumes of single chirality SWCNT in Sephacryl columns can take several days. Similarly, corona exchange by dialysis is slow and requires numerous changes of water baths over 24 to 32 h.<sup>[8,21]</sup> These methods may also have a low percent recovery of single chirality SWCNT, and are therefore not optimal for high-throughput screening of SWCNT coatings for sensor applications. However, recent developments in SWCNT separation have produced automated and scalable chromatographic SWCNT separation protocols, which have allowed routine suspensions of high purity single chirality SWCNT in SDS.<sup>[22]</sup> Here, we applied automatic separation protocols using a quantitative theory of adsorptive separation for electronic sorting of SWCNT of 6,5 and 7,6 chiralities.<sup>[14]</sup>

Another limitation for the production of ratiometric sensors is the inherent difficulty in exchanging SWCNT coronas. To produce a ratiometric sensor, one must selectively wrap one SWCNT chirality with a corona that is responsive to the analyte, and another SWCNT chirality with a corona that is either nonresponsive or responds opposite to the analyte signal. The difficulty lies in exchanging one SWCNT

corona, SDS in this case, for a corona that will enable a selective response to the target analyte with high exchange efficiency. As such, large-volume coating exchange processes for SDS-SWCNT remains a bottleneck for high throughput development of single chirality SWCNT sensors. The ability to separate SWCNT in scalable quantities combined with a novel and efficient, Rapid Corona Exchange for SWCNT (RACES), enables the production of ratiometric sensors to detect separate analytes using a single optical sensing platform.

In this work, we capitalize on these recent advances to create two distinct examples of ratiometric sensors, one for hydrogen peroxide (H<sub>2</sub>O<sub>2</sub>) and the other for nitric oxide (NO). Reactive oxygen and nitrogen species have been traditionally difficult to detect due to their rapid diffusivities and short lifetimes.<sup>[23,24]</sup> Therefore, there is significant interest in detecting these species with optical sensors. Furthermore, NO is a signaling molecule in plants<sup>[25]</sup> whereas H<sub>2</sub>O<sub>2</sub> is an indicator of oxidative stress that can damage the plant's photosynthetic machinery.<sup>[26]</sup> For each species, we identify unique corona phases that are selective to each analyte, and pair them with a corona phase that is largely invariant to that analyte by using RACES. The result, for each case, is a pair of SWCNT fluorescence emitters, where only one is modulated in response to an analyte and the other signal acts as a reference, allowing absolute calibration independent of overall intensity, a clear advance from a multichirality approach. Finally, we demonstrate the utility of our ratiometric sensor approach *in vivo* by detecting H<sub>2</sub>O<sub>2</sub> and NO in optically dense and biologically complex living plant tissues.

## 2. Results and Discussion

### 2.1. Suspension and Characterization of Poly-Coated Single Chirality SWCNT

Using single chirality SWCNT requires separation in SDS through columns of Sephacryl<sup>[13,14]</sup> followed by coating exchange of SDS with other species by dialysis.<sup>[21]</sup> Coating exchange by dialysis is slow, requiring numerous water bath changes,<sup>[8,21]</sup> sometimes resulting in low recovery of single chirality SWCNT. Therefore, dialysis is not optimal for preparative scale SWCNT suspensions. A novel technique for coating exchange of SDS single chirality SWCNT, RACES, allows rapid, and efficient suspension of single chirality SWCNT with a variety of molecules. After SWCNT separation by chirality in 5% SDS, the wrapping is added to the suspension of carbon nanotubes at a 10:1 mass ratio. During bath sonication, the methanol (MeOH) content of the mixture is increased via dropwise addition to more than 60% v/v. Increasing the MeOH concentration beyond the critical micelle concentration for SDS likely solubilizes SDS as a surfactant monomer, thereby enabling the wrapping species to encapsulate the SWCNT (**Figure 1a**). The result is a gradual SDS desorption with simultaneous adsorption of the new wrapping to the carbon nanotube surface. The protocol can be performed in a few hours with yields up to ≈71% depending on the chemical structure of the new wrapping (**Figure 1b–c**).

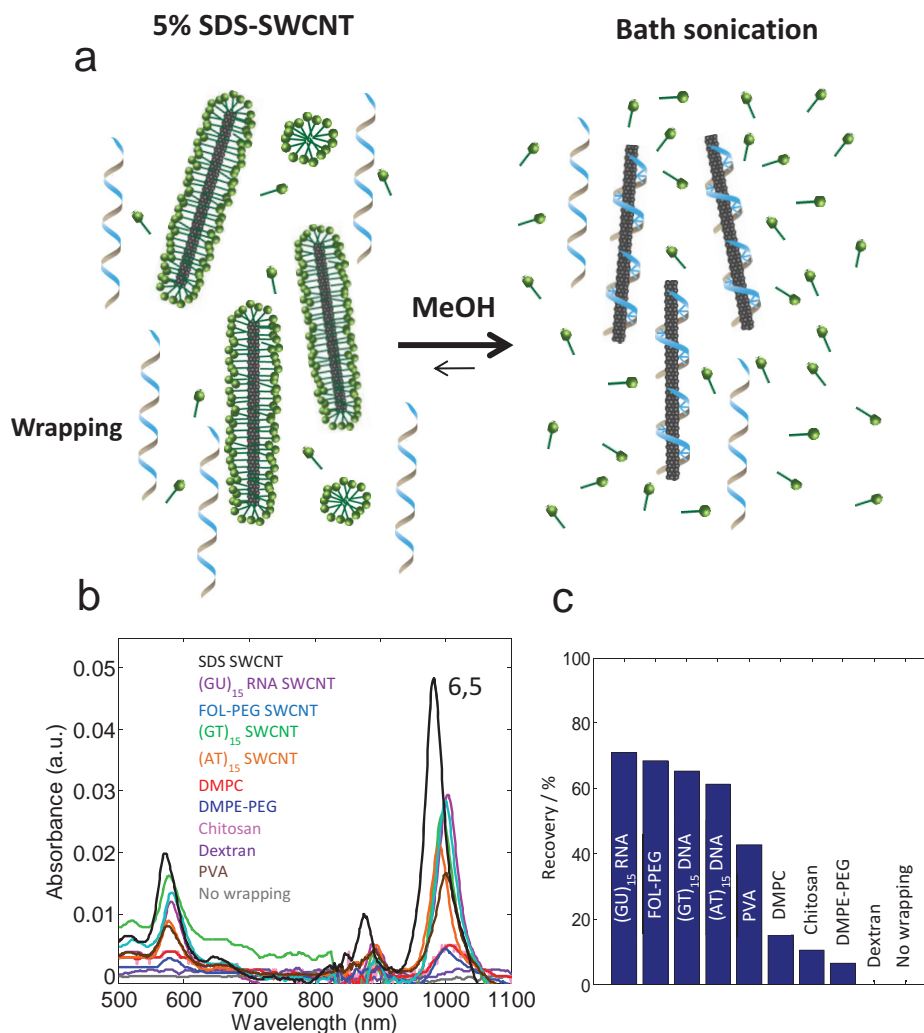


**Figure 1.** Method for rapid and efficient coating exchange of single chirality SWCNT by sonication. a) The free wrapping in solution adsorbs to SWCNT surface during bath sonication as MeOH is added dropwise. Addition of MeOH up to 60% v/v increases the critical micelle concentration of SDS from  $8.27$  to  $10.9 \times 10^{-3}$  M such that SDS falls into solution as a surfactant monomer. b) Absorption spectra of single chirality 6,5 SWCNT showing that coating exchange efficiency depends on the type of molecule. c) Percent recovery of 6,5 SWCNT after exchange of SDS with other coatings.

We predicted that the efficiency of the RACES SWCNT coating exchange would be dependent on the binding affinity of the exchanged molecule to the SWCNT surface. Wrappings high in functional groups that are likely to bind to the SWCNT surface via  $\pi$ -stacking, such as phenyl rings, should result in high-yield coating exchanges. We tested the exchange efficiency of RACES for a variety of different molecules as depicted in **Figure 2**. The exchange efficiency was determined by the percent recovery of SWCNT, as calculated by comparing initial and final concentrations of SWCNT based on the E11 peak of absorbance for 6,5 SWCNT. As expected, we found the highest exchange efficiency in RNA (71%), folate-polyethylene glycol (FOL-PEG) (65%), and DNA (61%) coatings, which are rich in aromatic groups (Figure 1b,c). In contrast, RACES has very low SWCNT recovery when SDS is exchanged with lipids such as 1,2-dimyristoyl-sn-glycero-3-phosphocholine (DMPC) (15%) and 1,2-dimyristoyl-sn-glycero-3-phosphoethanolamine-N-methoxy PEG (DMPE-PEG) (6%), due to

the low binding affinity of these polymers or surfactants to the SWCNT.

The high percentage of recovery of DNA, RNA and FOL-PEG is caused by cooperative effects, including the strong attraction between the aromatic rings and the SWCNT sidewalls, and the stabilization of the hydrogen bonding network between adjacent molecules. In addition, DNA or RNA may helically wrap SWCNT via  $\pi$ -interactions.<sup>[27]</sup> Polyvinyl alcohol (PVA) showed moderate percentage of recovery possibly due to the lack of aromatic groups and relatively neutral charge. However, PVA has a unique property of irreversible adsorption to hydrophobic surfaces, which is explained by polymer crystallization occurring concurrently with adsorption.<sup>[28]</sup> The hydrogen bonding network of PVA can additionally tighten the affinity between PVA and SWCNT. Chitosan is a weak base with a pKa value of D-glucosamine of about 6.2–7 and therefore is insoluble at neutral and alkaline pH values. To dissolve chitosan in water, we added acetic acid. In acidic conditions, the amine groups are protonated

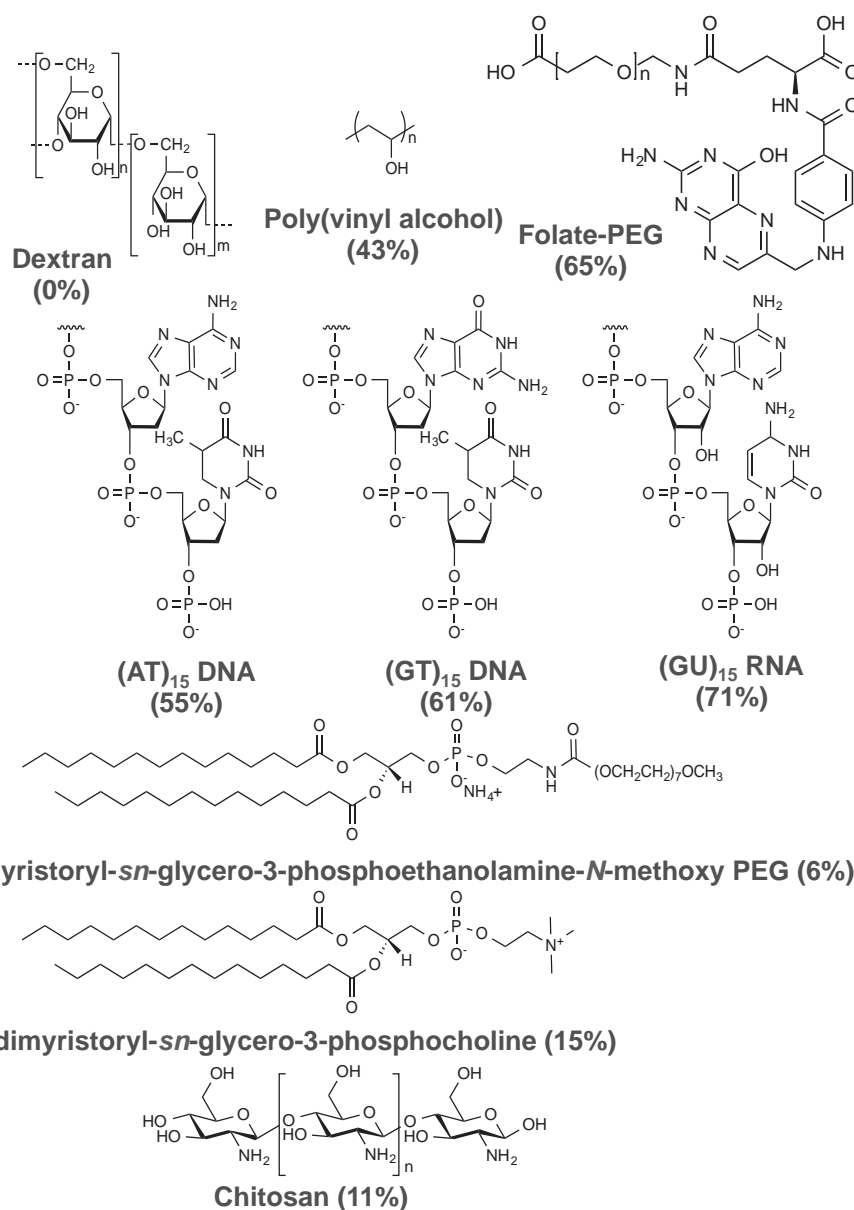


**Figure 2.** Chemical structures of molecules used for single chirality SWCNT coating exchange. Exchange recovery depends on the chemical structure of the molecules, with aromatic groups in DNA, RNA, and FOL-PEG enabling more efficient SWCNT coating exchange.

resulting in a soluble form of chitosan. Chitosan in solution exists in the form of a quasi-globular conformation stabilized by extensive intra- and intermolecular hydrogen bonding, which might provide weak attraction between chitosan and SWCNT.<sup>[29]</sup> The DMPC is a cationic surfactant that strongly interacts with anionic surfactants, such as SDS, thus affecting DMPC micelle formation around SWCNT.<sup>[30]</sup> Amphiphilic molecules containing long alkyl chains and PEG, like DMPE-PEG, can interact with SDS. The structure of DMPE-PEG is preserved up to an SDS concentration that coincides with its critical micelle concentration.<sup>[31]</sup> Therefore, our surfactant exchange method leads to low recovery percentage of SWCNT with DMPE-PEG. Dextran is a complex, branched glucan composed of chains of varying lengths. The binding between SWCNT and dextran is limited solely to its hydrophobic interaction with the central part of the dextran chain.

Dextran-SWCNT complexes have been previously made by the traditional method of adding solid SWCNT to aqueous dextran as we mentioned above.<sup>[32]</sup> However, our method requires the addition of methanol that causes dextran precipitation and thereby no recovery of Dextran-SWCNT.

## 2.2. SWCNT Ratiometric Detection of Free Radicals In Vitro

We selected two different analytical systems to address using our ratiometric detection approach. In system 1 ( $\text{H}_2\text{O}_2$  detection platform), we used ss(GT)<sub>15</sub> DNA wrapped 7,6 SWCNT (Emission = 1131 nm) that quenches in the presence of  $\text{H}_2\text{O}_2$ , combined with 6,5 ss(AT)<sub>15</sub> DNA SWCNT (Emission = 984 nm) that is largely invariant to  $\text{H}_2\text{O}_2$ . The result is a pair of emission wavelengths that can determine changes in  $\text{H}_2\text{O}_2$



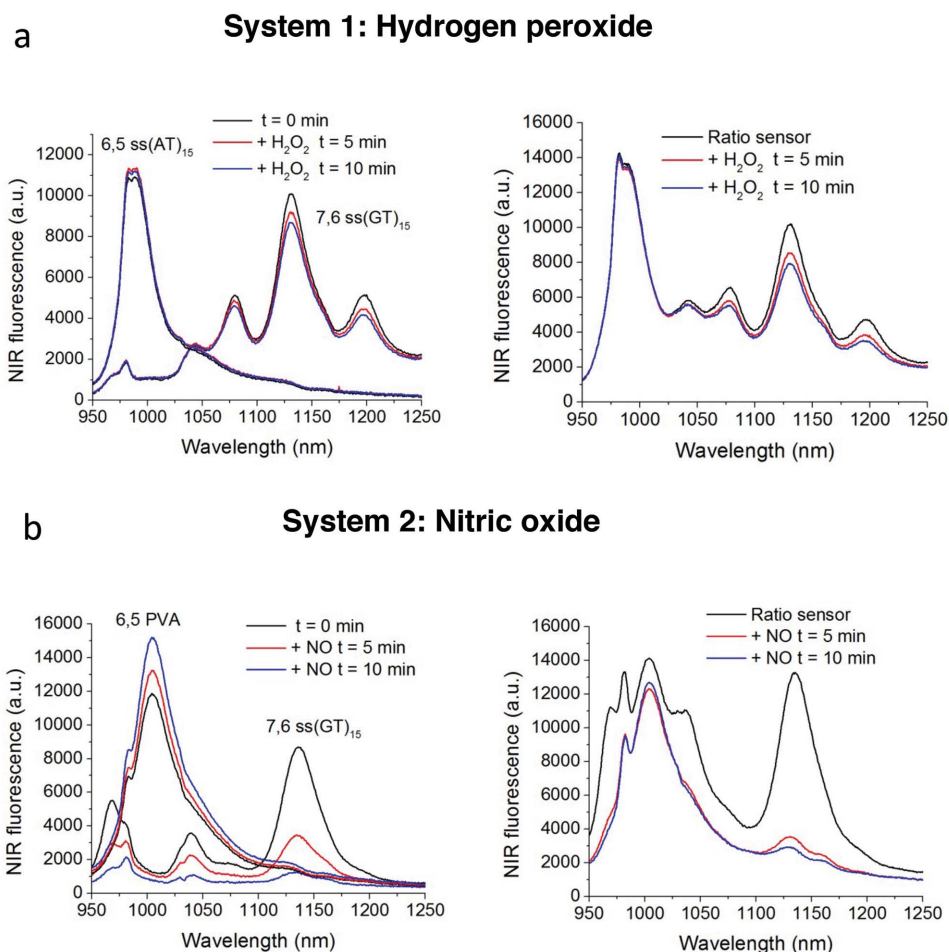


**Figure 3.** Ratiometric sensor response to hydrogen peroxide and nitric oxide in vitro. a) Changes in the near-infrared fluorescence of 6,5 ss(AT)<sub>15</sub>, 7,6 ss(GT)<sub>15</sub> SWCNT, and combined spectrum in the presence of hydrogen peroxide ( $100 \times 10^{-6}$  M) (system 1). b) Response of 6,5 PVA, 7,6 ss(GT)<sub>15</sub> SWCNT, and combined near-infrared spectrum to nitric oxide ( $500 \times 10^{-6}$  M) (system 2). SWCNT suspensions were excited with a 785 nm laser.

independent of absolute intensity. As expected, the NIR fluorescence of 6,5 SWCNT coated with ss(AT)<sub>15</sub> was not affected by the presence of  $100 \times 10^{-6}$  M H<sub>2</sub>O<sub>2</sub> (Figure 3a). In contrast, 7,6 ss(GT)<sub>15</sub> SWCNT fluorescence was quenched by  $\approx 20\%$  within 10 min of addition of H<sub>2</sub>O<sub>2</sub> (Figure 3a and Figure 4a). Previously, our group demonstrated that SWCNT coated in DNA act as selective, real time sensors of H<sub>2</sub>O<sub>2</sub>, along with calibration curves of NIR signal versus H<sub>2</sub>O<sub>2</sub> concentration.<sup>[20,33]</sup> The changes in NIR fluorescence were similar when the single chirality SWCNT 6,5 and 7,6 were tested in separate suspensions in the presence of H<sub>2</sub>O<sub>2</sub>, and combined in one solution as a ratiometric sensor (Figure 3a). In system 2 (NO detection platform), we used 6,5 PVA SWCNT (Emission = 1004 nm) as the chirality invariant to NO mixed with ss(GT)<sub>15</sub> DNA wrapped 7,6 (Emission = 1135 nm) SWCNT for NO sensing via a quenching response (Figure 3b). This free radical has been previously shown to dramatically and reversibly decrease the NIR fluorescence of a mix of DNA wrapped SWCNT (Unydim) and at the single-molecule scale in vitro<sup>[34]</sup> and more recently in leaves of living plants in vivo.<sup>[19]</sup> Conversely, PVA is among one of very few polymers able to prevent the interaction of NO with the carbon nanotube surface.<sup>[34]</sup> A calibration curve for the DNA SWCNT fluorescence in response to different concentrations of NO

in solution has also been reported previously.<sup>[34]</sup> Combined in a ratiometric sensor, the NIR fluorescence of 6,5 PVA SWCNT did not significantly change as expected in the presence of  $500 \times 10^{-6}$  M NO while 7,6 ss(GT)<sub>15</sub> SWCNT exhibited a strong decrease in NIR fluorescence (Figure 3b). The largest NIR response of 7,6 ss(GT)<sub>15</sub> SWCNT occurred a few minutes after the addition of NO (Figure 4b). The slight variations in NIR fluorescence in the reference 6,5 SWCNT and analyte sensing 7,6 SWCNT are likely due to noise in the experimental system. These fluorescence variations may highlight the limits of detection of the ratiometric sensor under in vitro conditions.

Together, our results demonstrate that ratiometric detection of free radicals using SWCNT is possible. By coating single chirality SWCNT with specific wrappings, we built a ratiometric platform that can report on the presence of target analytes while monitoring signal interfering factors in vivo such as dilution effects, local nanoparticle concentration, signal depth, and other biomolecules. This platform could lead to more selective SWCNT-based sensors, as each chirality coated with a different wrapping has the potential to create a unique spectral signature in response to an analyte. We envision expanding this platform to the use of multiple SWCNT chiralities, where each chirality will be functionalized with a

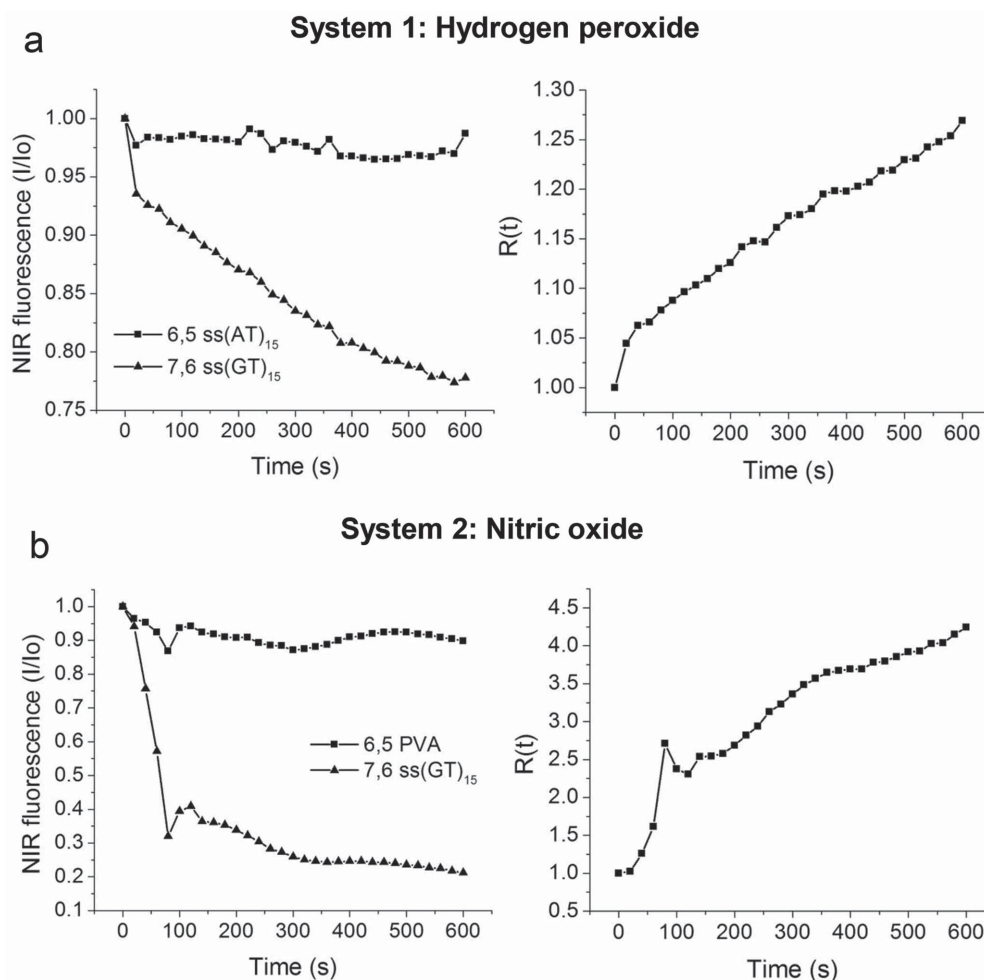


**Figure 4.** Temporal changes in 6,5 and 7,6 SWCNT peak intensity and ratio of intensity ( $R$ ) after addition of  $\text{H}_2\text{O}_2$  and  $\text{NO}$ . a) In the presence of  $100 \times 10^{-6} \text{ M}$   $\text{H}_2\text{O}_2$ , the NIR fluorescence of 6,5 ss(AT)<sub>15</sub> SWCNT remains relatively constant while 7,6 ss(GT)<sub>15</sub> SWCNT fluorescence quenches steadily. b) The addition of  $500 \times 10^{-6} \text{ M}$  of  $\text{NO}$  does not affect 6,5 PVA SWCNT fluorescence but strongly reduces 7,6 ss(GT)<sub>15</sub> SWCNT intensity. Temporal patterns of  $R(t)$  in response to  $\text{H}_2\text{O}_2$  and  $\text{NO}$  represent the normalized intensity peak changes of 6,5 and 7,6 SWCNT, calculated according to Equation (1). SWCNT suspensions were excited with a 785 nm laser.

unique moiety. This multiplexing approach may dramatically improve the selectivity of SWCNT sensing platforms, particularly in nonhomogenous and chemically complex living tissues. With a method analogous to that used for visible dye based ratiometric systems,<sup>[35]</sup> we calculate the change of ratio of intensity ( $R$ ) over time for  $\text{H}_2\text{O}_2$  and  $\text{NO}$  (Figure 4). We define  $R$  as the normalized signal difference between the 6,5 chirality and the 7,6 chirality as

$$R(t) = \frac{I_{6,5}^{\text{norm}}(t)}{I_{7,6}^{\text{norm}}(t)} \quad (1)$$

where

$$I_{6,5}^{\text{norm}}(t) = \frac{I_{6,5}(t)}{I_{6,5}(0)} \quad (2)$$

and,

$$I_{7,6}^{\text{norm}}(t) = \frac{I_{7,6}(t)}{I_{7,6}(0)} \quad (3)$$

Figure 4a shows the dependence of the intensity ratios of absorbance for  $I_{6,5}^{\text{norm}}(t)$  at 984 nm to that of  $I_{7,6}^{\text{norm}}(t)$  at 1131 nm as a function of time for a response to  $\text{H}_2\text{O}_2$ . The  $R(t)$  values increase monotonically from  $t = 0$  to  $t = 600$  s. The linear behavior of the  $\text{H}_2\text{O}_2$  ratiometric sensor beyond  $t = 20$  s can be attributed to the fact that the binding sites of SWCNT are still unsaturated at the relatively low peroxide concentrations utilized, which implies that the  $\text{H}_2\text{O}_2$  binding probabilities are unchanging. The intensity ratios of  $I_{6,5}^{\text{norm}}(t)$  at 1004 nm to that of  $I_{7,6}^{\text{norm}}(t)$  at 1135 nm as a function of time for a response to  $\text{NO}$  are similarly shown in Figure 4b. The  $R(t)$  values increased with time from  $t = 0$  to  $t = 600$  s. The transient response in Figure 4 is diffusion limited, as the measurements were conducted in unstirred wells of a 96 well-plate. The slow transient reflects the diffusion of  $\text{NO}$  and  $\text{H}_2\text{O}_2$  into the total volume of the well. The observed non-monoatomic nature of  $R$  for  $\text{NO}$  at short times ( $t < 120$  s) could be due to variability in ligand binding or noise in the experimental system. These results indicate that  $R(t)$  change can be used to monitor the binding of  $\text{H}_2\text{O}_2$  or  $\text{NO}$  on 6,5 and 7,6 SWCNT.

### 2.3. Spatial and Temporal Patterns of Ratiometric Sensor Fluorescence in Living Tissues

Dyes with fluorescence in visible wavelengths have been commonly used as sensors for  $\text{H}_2\text{O}_2$ <sup>[36,37]</sup> and  $\text{NO}$ .<sup>[24,37–39]</sup> Although these fluorophores enable imaging with cellular resolution, in real time, they present a set of complex problems for in vivo applications.<sup>[40,41]</sup> Amplex red is widely used for imaging low concentrations of  $\text{H}_2\text{O}_2$  but has rarely been shown to work in living tissues due to its quick photodegradation.<sup>[42]</sup> The cell permeable 2',7'-dichlorodihydrofluorescein diacetate ( $\text{H}_2\text{DCF-DA}$ ) dye has been demonstrated to detect  $\text{H}_2\text{O}_2$  in living organisms despite its relatively nonselectivity to reactive oxygen species (ROS)<sup>[23]</sup> and susceptibility to photo-oxidation and photobleaching.<sup>[40]</sup> Imaging of  $\text{NO}$  in living systems has been performed with diamionofluoresceins with the disadvantage that their fluorescein chromophore is responsive to changes in  $\text{pH}$ <sup>[43]</sup> and reacts with dehydroascorbic and ascorbic acid.<sup>[41]</sup>

Plants are optically dense living organisms due to thick tissues and photosynthetic pigments, making it difficult to detect analytes in vivo.  $\text{H}_2\text{O}_2$  can be generated in plants by the leaf photosynthetic pigments<sup>[44]</sup> while  $\text{NO}$  can be produced by multiple metabolic pathways.<sup>[25]</sup> SWCNT are well suited for in vivo detection of trace levels of analytes with short lifetimes such as  $\text{H}_2\text{O}_2$  and  $\text{NO}$  in plants. Furthermore, SWCNT fluorescence in the NIR in which living tissues are relatively transparent, do not photobleach, and allow detection at the single particle level.<sup>[19,34]</sup> We tested the response of two distinct SWCNT ratiometric sensors,  $\text{H}_2\text{O}_2$  and  $\text{NO}$ , in real time, inside

sections of leaves of living plants. We monitored the NIR response of the 6,5 ss(AT)<sub>15</sub> and 7,6 ss(GT)<sub>15</sub> SWCNT ratio sensor for  $\text{H}_2\text{O}_2$  and the NIR response of 6,5 PVA and 7,6 ss(GT)<sub>15</sub> SWCNT ratio sensor for  $\text{NO}$ . Each SWCNT ratio sensor was delivered inside cross sections of leaves mounted on a microfluidic perfusion platform (**Figure 5**). As we have previously shown, SWCNT can localize in intracellular and extracellular compartments in leaf tissues.<sup>[19]</sup> Leaf sections were washed with phosphate buffered saline (PBS) to remove free SWCNT not-incorporated into the leaf sections. Upon exposure to  $\text{H}_2\text{O}_2$ , the 6,5 ss(AT)<sub>15</sub> SWCNT NIR fluorescence slightly increased by  $\approx 11\%$  while the 7,6 ss(GT)<sub>15</sub> SWCNT quenched (**Figure 6a**). The changes in NIR fluorescence of the 6,5 and 7,6 SWCNT occurred rapidly, in less than 50 s, upon exposing the leaf sections to the ROS. Similarly,  $\text{NO}$  in solution induced no response in 6,5 PVA-SWCNT but led to a decrease in NIR fluorescence of the 7,6 ss(GT)<sub>15</sub> SWCNT of 50% (**Figure 7a**). The changes in SWCNT fluorescence of 7,6 ss(GT)<sub>15</sub> SWCNT were recorded after less than 50 s after exposure to  $\text{NO}$ .

The NIR fluorescence response of our SWCNT ratio sensors to  $\text{H}_2\text{O}_2$  and  $\text{NO}$  in leaf sections showed similar trends relative to experiments carried out in vitro. However, the NIR quenching signal inside leaves for the 7,6 chiralities in both ratio sensors was not as steep as under in vitro conditions. This is most likely due to the passivation of SWCNT surfaces with other biomolecules found in plant tissues during the infiltration through the leaf cross sections. This can be corrected by calibration of the sensor after exposure to tissue components. As a negative control, the perfusion of water on the leaf surface caused no noticeable changes in the

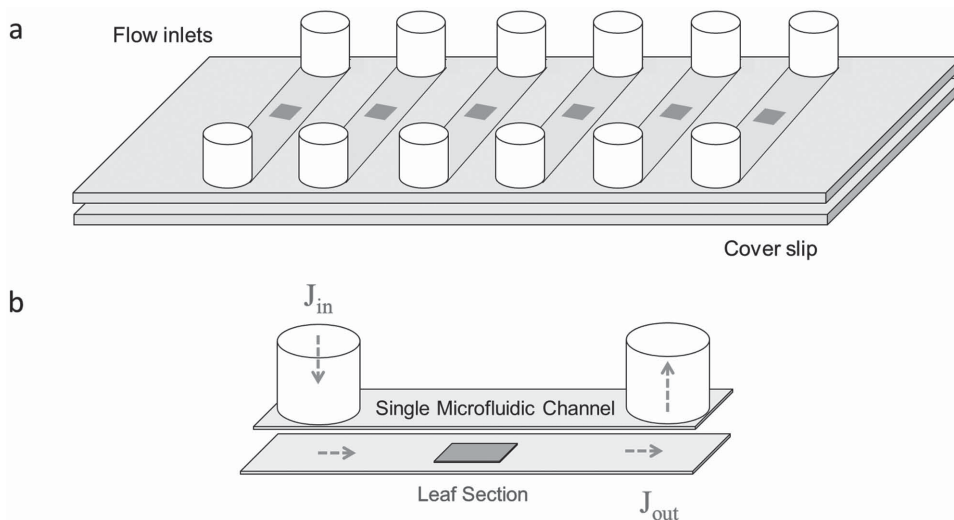


**Figure 5.** Imaging of SWCNT ratiometric response to free radicals in vivo was performed in *Arabidopsis thaliana* leaf sections ( $\approx 2 \times 2$  mm) mounted on a Ibidi  $\mu$ -Slide (Ibidi, VI 0.4). a) A glass coverslip (No. 1, Fisher Scientific) placed at the bottom of the Ibidi  $\mu$ -Slide created six individual flow channels with one leaf section per channel, and adhered to the Ibidi slide such that the leaf sections remained immobilized between the microfluidic slide surface and coverslip. b) Schematic of one of the six microfluidic slides. 50  $\mu\text{L}$  of PBS buffer was added to each channel into the inlet ( $J_{\text{in}}$ ). The buffer ensured the leaf section was properly immobilized. 50  $\mu\text{L}$  of ratiometric SWCNT sensor made by mixing approximately equal concentrations of each the 6,5 and 7,6 chirality of polymer-SWCNT in PBS buffer was added to the flow inlet ( $J_{\text{in}}$ ), and an equal volume was removed from the flow outlet ( $J_{\text{out}}$ ). The suspension was allowed to incubate with leaf sections for 3 h to enable SWCNT assembly into the leaf tissue. Subsequently, 50  $\mu\text{L}$  of PBS buffer was perfused through each channel through the inlet ( $J_{\text{in}}$ ) followed by removal of this volume from the outlet ( $J_{\text{out}}$ ) to extract SWCNT not permeated into leaf tissue. Finally, 50  $\mu\text{L}$  of a dissolved  $\text{NO}$  or  $\text{H}_2\text{O}_2$  solution was infused into the microfluidic channel through the inlet ( $J_{\text{in}}$ ), exposing the leaf section with SWCNT sensors to the free radicals in solution.



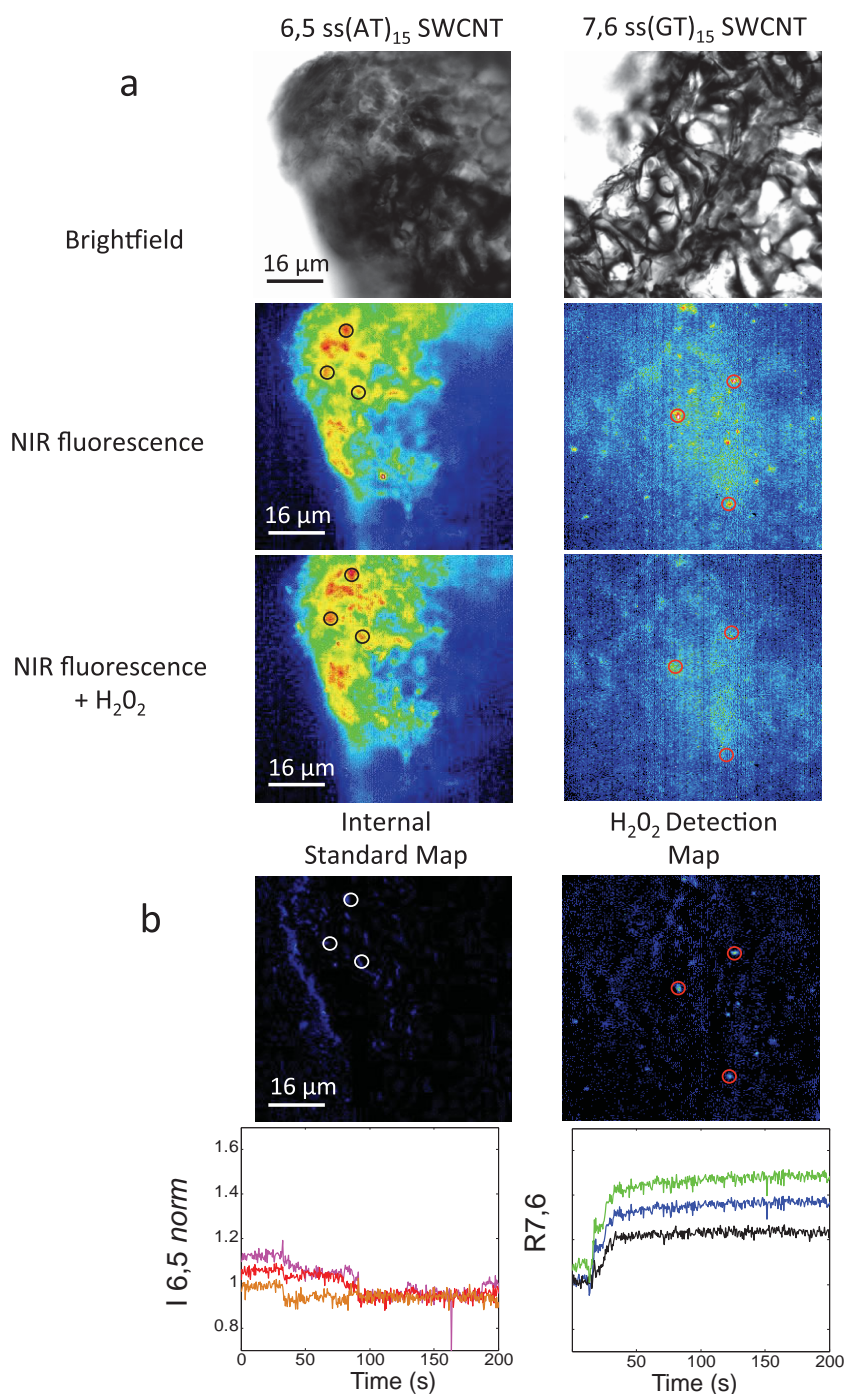


**Figure 6.** Ratiometric sensor response to hydrogen peroxide in vivo inside leaves. Leaf sections infiltrated with a 6,5 ss(AT)<sub>15</sub> and 7,6 ss(GT)<sub>15</sub> ratio sensor for H<sub>2</sub>O<sub>2</sub>, where each chirality is independently imaged with a 785 nm excitation source. a) From top to bottom, images of ratiometric sensor-infiltrated leaves in bright-field, in the NIR prior to addition of H<sub>2</sub>O<sub>2</sub>, in the NIR upon addition of 20 μL of 10 × 10<sup>-3</sup> M H<sub>2</sub>O<sub>2</sub>. b) Maps of internal standard,  $I_{6,5}^{\text{norm}}$ , and H<sub>2</sub>O<sub>2</sub> detection determined by the NIR intensity change in the leaf section that is the difference in intensity pre and post H<sub>2</sub>O<sub>2</sub> addition. Traces of internal standard and ratiometric response,  $R_{7,6}$ , are shown as a function of time.

NIR fluorescence of 6,5 PVA-SWCNT, 6,5 ss(AT)<sub>15</sub>-SWCNT, and 7,6 ss(GT)<sub>15</sub>-SWCNT (Figure S1a,b, Supporting Information). Together, these results indicate that the observed changes in SWCNT fluorescence are a result of the reaction of H<sub>2</sub>O<sub>2</sub> and NO with the carbon nanotube surface.

solutions throughout the entire leaf section. Therefore, we can presume that the individual SWCNT chiralities are responding to the same free radical conditions upon perfusion. Analysis of over 60 SWCNT sensors in plant tissues show that, for NO, the reference 6,5 chirality remains largely

We independently monitored a spatio-temporal response of each SWCNT chirality, 7,6 and 6,5, from within the tissues of infiltrated leaves. SWCNT-infiltrated leaf sections were immobilized within a microfluidic chamber, and the entire leaf tissue was exposed to solubilized NO or H<sub>2</sub>O<sub>2</sub>. We calculated our in vivo ratiometric response as represented by Equation (1) as the time-dependent change in the ratio of intensities between the initial 6,5 chirality intensity, which remains relatively invariant, and the quenching 7,6 chirality, which is responsive to our analytes (Figure 6 and 7). For our in vivo imaging, we included a correction factor,  $\rho$ , to normalize the initial difference in the intensity between the two chiralities

$$R_{7,6}(t) = \rho \frac{I_{6,5}(0)}{I_{7,6}(t)} \quad (4)$$

Additionally, we calculated the internal reference variable  $I_{6,5}^{\text{norm}}(t)$  as the time-dependent response of our reference chirality, the 6,5 SWCNT, in the presence of our analytes by including in Equation (2) the correction factor  $\rho$ :

$$I_{6,5}^{\text{norm}}(t) = \rho \frac{I_{6,5}(t)}{I_{6,5}(0)} \quad (5)$$

In the presence of H<sub>2</sub>O<sub>2</sub>, we observe a gradual increase of  $R_{7,6}(t)$  for 7,6 ss(GT)<sub>15</sub> SWCNT (Figure 6b), as expected from our in vitro experiments. There is relatively little change in  $I_{6,5}^{\text{norm}}(t)$  in the leaf tissues after exposure to H<sub>2</sub>O<sub>2</sub>, which is consistent with the in vitro characterization of our H<sub>2</sub>O<sub>2</sub> ratiometric sensor. Likewise, when our leaf sections were in the presence of NO, we observed a gradual increase of  $R_{7,6}(t)$  for 7,6 ss(GT)<sub>15</sub> SWCNT (Figure 7b), as expected from our in vitro experiments. Our internal reference for the NO ratio sensor,  $I_{6,5}^{\text{norm}}$ , remains invariant in the presence of NO throughout the course of the experiment. Although imaging was performed at different locations of the leaf tissue for each chirality, the exposure to NO and H<sub>2</sub>O<sub>2</sub> with our microfluidic chamber ensured homogeneous perfusion of these free radical

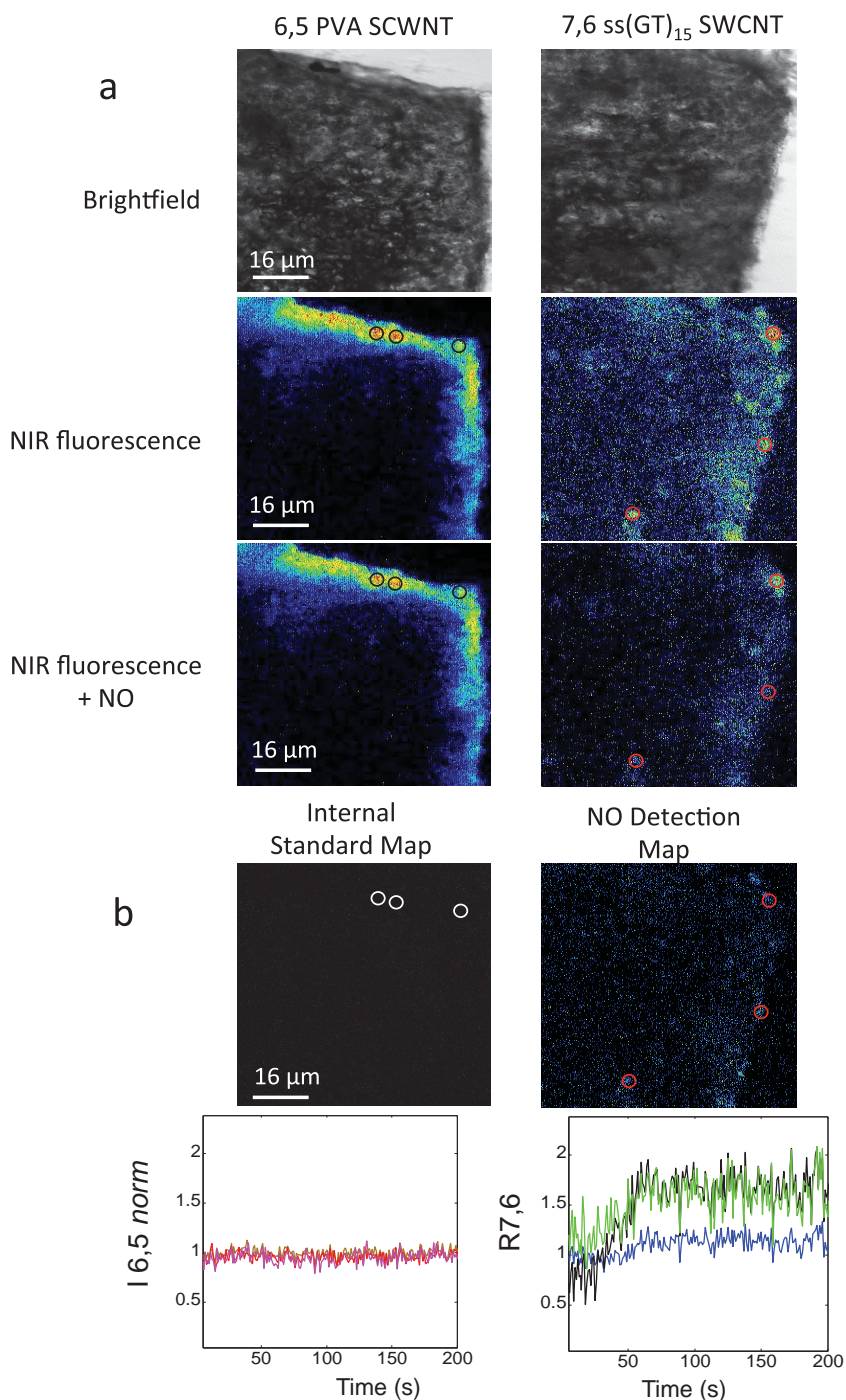


**Figure 7.** Ratiometric sensor response to nitric oxide in vivo inside leaves. Leaf sections infiltrated with a 6,5 PVA and 7,6 ss(GT)<sub>15</sub> ratio sensor for NO, where each chirality is imaged independently with a 785 nm laser excitation. a) From top to bottom, images of ratiometric sensor-infiltrated leaves in bright-field, in the NIR prior to addition of NO, in the NIR upon addition of 20 μL of 50 × 10<sup>-3</sup> M NO. b) Maps of internal standard,  $I_{6,5}^{norm}$ , and NO detection determined by the NIR intensity change in the leaf section that is the difference in intensity pre and post NO addition. Traces of internal standard and ratiometric response,  $R_{7,6}$ , are shown as a function of time.

invariant ( $(I-I_0)/I_0 = -0.010 \pm 0.008$ ; mean  $\pm$  SE), whereas the NO-responsive 7,6 chirality quenches upon NO perfusion ( $(I-I_0)/I_0 = -0.362 \pm 0.042$ ; mean  $\pm$  SE). Likewise, for H<sub>2</sub>O<sub>2</sub>, the reference 6,5 chirality remains largely invariant

( $(I-I_0)/I_0 = -0.013 \pm 0.009$ ; mean  $\pm$  SE), whereas the H<sub>2</sub>O<sub>2</sub>-responsive 7,6 chirality quenches upon H<sub>2</sub>O<sub>2</sub> perfusion ( $(I-I_0)/I_0 = -0.246 \pm 0.024$ ; mean  $\pm$  SE).

The observed ratiometric signal within leaves saturate around 50 s instead of the more than 600 s observed in vitro. These timescale differences in the sensor response inside the leaves relative to the experiments in vitro are related to the volume of the chamber around the sensor and the transport rates of the free radicals (see the Experimental Section). The rapid flow velocities of the leaf microfluidic chamber contribute greatly to the fast response of the sensors. Unlike the in vitro experiment where there is no mixing, only diffusion in the well, in the leaf microfluidic chamber we deliver the free radicals in solution into the sensor location very quickly by convective flow. It is also important to note that the intensity quenching saturation of the leaf is only a small fraction of the in vitro experiment. The quenching time in vitro at an equivalent 15% quenching occurs in  $\approx$ 50 s, similar to the in vivo response, and likely due to the degradation of the reactive species as it travels through the leaf tissue. The results of our ratiometric sensing experiments in leaf sections highlight the importance of having a dual-SWCNT signal for in vivo sensing. It can be difficult to attribute sensor specificity to an analyte in complex living tissues where changes in sensor distribution, scattering media, and presence of other biomolecules can modify the optical response. In particular, small reactive molecules such as reactive oxygen and nitrogen species are notoriously difficult to monitor in vivo due to their short lifetimes and fast diffusivities. Our dual-chirality ratiometric sensor provides a reference 6,5 SWCNT chirality that remains invariant in vivo despite the presence of factors not associated with the intended analyte. Meanwhile, the quenching response of the 7,6 SWCNT chirality monitors the analyte's presence. Therefore, this ratiometric sensing platform is a powerful tool for improving the detection of analytes in dynamic and chemically diverse environments.

Other nanosensors for detecting free radicals such as NO have been reported previously,<sup>[19,45,46]</sup> but only SWCNT-based sensors have been demonstrated to respond in living plants. SWCNT show a remarkable ability to penetrate through the walls of plant cells<sup>[19,47]</sup> having pores of less than a few nanometers wide.<sup>[48]</sup>



Therefore the applicability of many nanosensors is limited based on their size. Furthermore, SWCNT near-infrared fluorescence allows deeper imaging into living tissues than other sensing platforms that are based on visible fluorescence or Raman. SWCNT-based sensors also offer advantages for in vivo sensing applications such as high photostability and fluorescence quantum efficiency.<sup>[17]</sup> SWCNT ratiometric sensors have the potential to enhance sensitivity to the single particle level and enable multiplexing with different SWCNT chiralities. Using the fabrication mechanisms outlined in this study, a variety of SWCNT ratiometric sensors could be built for detecting biomolecules in complex environments, including dopamine,<sup>[18]</sup> glucose,<sup>[49]</sup> insulin,<sup>[50]</sup> and singlet oxygen,<sup>[20]</sup> among others.

Our development and application of ratiometric sensors can create plants that act as detectors of both NO and H<sub>2</sub>O<sub>2</sub>, which are key regulators of plant metabolism, and in the case of NO a pollutant of the environment. The reversibility of this sensor,<sup>[34]</sup> combined with the year-long timescales for which it can detect reactive species<sup>[17]</sup> could enable multiple applications. We envision that our nanosensor-interfaced plants with single chirality SWCNT ratiometric sensors will make a more robust platform for biochemical monitoring under changing field conditions. For instance, multiplexing the NIR signal from nanosensor-interfaced plants could enable detection of SWCNT fluorescence remotely with stand-off devices such as NIR cameras, even to the midst of complex environmental, chemical, and optical conditions. Future stand-off detection of analytes could rely on SWCNT chiralities able to report variations in NIR signal due to excitation intensity, angle of emission, and transmittance in the environment. We have recently shown that plants interfaced with SWCNT can be augmented to function as optical sensors.<sup>[19]</sup> Plants can offer a unique capability of self-powered accumulators of chemicals from the environment that are difficult to detect. Our nanobionic approach of providing plants with novel or augmented functions using nanomaterials will lead to plants that act as inconspicuous photonic sensors reporting the plant metabolic status or a variety of biochemicals in the environment.

### 3. Conclusion

The development of SWCNT ratiometric sensors was facilitated by a rapid and efficient coating exchange, RACES, for single chirality SWCNT. This technique enabled high throughput production of 6,5 and 7,6 SWCNT sensors coated in corona phases individually functionalized to produce unique optical signals in the presence of free radicals. We were successful in building two double chirality SWCNT ratiometric sensors: one for H<sub>2</sub>O<sub>2</sub> and another for NO. We show the utility of our ratiometric sensing platform by detecting each of these analytes in living plant tissues. The response of our ratiometric sensors in leaves was similar to in vitro tests, demonstrating the robustness of our SWCNT-based sensor approach for biological research applications. We propose that expanding SWCNT ratiometric platforms to multiple chiralities coated in diverse wrappings will create nanosensors with exquisite selectivity and sensitivity. This

fluorescence response has the potential to create a unique and multiplexed SWCNT spectral signature for each analyte while incorporating a nonresponsive reference signal, enhancing sensor quantification in living tissues.

### 4. Experimental Section

*Carbon Nanotube Suspension and Characterization:* The 6,5 SDS SWCNT were separated as previously reported by our group.<sup>[13]</sup> The 7,6 SDS-SWCNT suspension protocol was developed using a quantitative theory of adsorption separation of SWCNT.<sup>[14]</sup> In brief, SWE<sup>NT</sup>® SG76 SWCNT (100 mg, Southwest nanotechnologies) were suspended in 2% SDS (100 mL) by ½" tip sonication at 10 W for 13.5 h. The suspension was ultracentrifuged for 4 h at 32000 RCF and 90% of the supernatant was collected. Then the SWCNT solution (70 mL) was filtered through Sephacryl columns (14 mL) previously equilibrated in SDS 2% (Columns 1–10), 1.5% (Columns 10–15) and 1% (Columns 15–20) at a flow rate of 3 mL min<sup>-1</sup> (Figure S2, Supporting Information). After passing the suspension through each column, the SWCNT adsorbed to the Sephacryl were eluted in 5% SDS by maintaining the flow at 5 mL min<sup>-1</sup>. Fluorescence spectra for 6,5 and 7,6 SDS SWCNT varied slightly after each separation due to differences in SWCNT suspension purity.

*Rapid Corona Exchange for SWCNT (RACES):* Single-chirality SDS-SWCNT (2.5 mL) were bath sonicated for 60 min, followed by 1 h of centrifugation at 16 000 g to remove remaining SWCNT bundles. The SDS-SWCNT supernatant from the centrifugation process was transferred to a 5 mL glass vial and 10x mass excess of wrapping relative to SWCNT was added. The SDS-SWCNT mixture was mixed via Pasteur pipetting then bath sonicated for 30 min. Subsequently, methanol (3.5 mL) was added dropwise, during which the mixture was removed from the bath sonicator, capped, and mixed by inversion after the addition of every 0.5 mL of methanol to ensure mixture of lower-density methanol with the higher-density SWCNT solution. This process allows SDS to solubilize, and enables the accompanying wrapping to suspend the SWCNT. The stability of the suspension was verified by centrifugation at 16 000 g for 10 min. The preparation was washed in 5–10 cycles of 1 min each using a 100 K Amicon centrifuge filter (Millipore) at 500–1000 rpm, depending on the wrapping. The final suspension was re-suspended by mixing with a Pasteur pipette to its original volume of 2.5 mL in deionized water.

*SWCNT Ratiometric Sensor Response to Nitric Oxide and Hydrogen Peroxide In Vitro:* The NIR fluorescence of the SWCNT ratio sensor was monitored from 950 to 1250 nm under excitation of a 785 nm Invictus photodiode laser (Kaiser) with a modified Axiovision Zeiss microscope (×20 objective) attached to an OMV InGaAs linear array spectrometer (Princeton Instruments). Single chirality SWCNT 6,5 and 7,6 were mixed in a 300 μL well (BD falcon 96 well-plate) to reach approximately similar peaks of intensity at 980–1005 and 1130–1135 nm, respectively. The sharp NIR peak around 980 nm for both chiralities 6,5 and 7,6 corresponds to the characteristic 2D SWCNT Raman signal (2600–2700 cm<sup>-1</sup>) from the excitation at 785 nm. Changes in NIR fluorescence intensity were recorded every 20 s for 10 min after adding H<sub>2</sub>O<sub>2</sub> and NO at 1:100 volume ratio. Final concentration of H<sub>2</sub>O<sub>2</sub> and NO were 100 × 10<sup>-6</sup> M and 500 × 10<sup>-6</sup> M, respectively. As negative controls,

we show that the addition of water instead of free radicals causes minor changes in the NIR fluorescence of 6,5 PVA, 6,5 ss(AT)<sub>15</sub>, and 7,6 ss(GT)<sub>15</sub> SWCNT in vitro (Figure S3a–c, Supporting Information). We chose a higher working concentration of NO and H<sub>2</sub>O<sub>2</sub> to compensate for the instability of these molecules, thus avoiding their complete degradation prior to reaching our sensor for in vivo experiments in leaf tissues.

**SWCNT Leaf Infiltration:** Arabidopsis thaliana leaf sections were taken by excising  $\approx 2 \times 2$  mm sections of leaf tissue with a razor blade. Six leaf sections were mounted along an Ibidi  $\mu$ -Slide (Ibidi, VI 0.4). A glass coverslip (No. 1, Fisher Scientific) was placed on top to create six individual flow channels with one leaf section per channel. A solution of 50  $\mu$ L of PBS buffer was added to each channel. A ratiometric SWCNT sensor was made by mixing approximately equal concentrations of each the 6,5 and 7,6 chirality of wrapped SWCNT. A suspension of ratiometric sensor (50  $\mu$ L) was added to each channel and allowed to incubate with leaf sections for 3 h to enable SWCNT diffusion into the leaf tissue. Then PBS buffer (50  $\mu$ L) was perfused through each channel to remove SWCNT that had not permeated into leaf tissue.

**Imaging SWCNT Ratio Sensor In Vivo Inside Leaves in Real Time:** Ratiometric sensing videos were recorded in an Axio Vision inverted microscope (Zeiss) and imaged with an InGaAs OMA V 2D array detector (Princeton Instruments). The autofluorescence of chloroplast pigments in leaf sections was avoided by using a 785 nm Invictus photodiode laser (Kaiser) excitation source that is off-resonance with these pigments. Imaging of 6,5 chirality SWCNT was accomplished by using a 935/170 nm BrightLine single-band bandpass filter (Semrock, FF01--935/170--25) to capture only the emission of the 6,5 chirality SWCNT. Imaging of the 7,6 SWCNT was performed by using a 1100 nm long pass emission filter (Chroma) to capture the peak of emission of this SWCNT chirality. There was no emission overlap between these two filter sets. Leaf sections were infiltrated as explained above with 6,5 and 7,6 ratio sensors, mounted within an Ibidi VI 0.4 slide (Figure 5), and fluorescence recorded at 0.5 s exposure per frame. We imaged each chirality within a leaf section independent of the other chirality, and monitored the change in the SWCNT intensity as a function of time upon addition of analyte. For the 7,6 chirality, we monitored its time-dependent response,  $R_{7,6}$ , against an invariant intensity from the reference 6,5 chirality at the initial experimental timepoint. For the 6,5 chirality, we monitored its time-dependent response,  $I_{6,5}^{\text{norm}}$ , against the initial intensity from the 6,5 chirality, to ensure that the 6,5 chirality was indeed invariant upon addition of the analyte.

A relationship between the volume of the chamber around the sensor, the transport rates, and the change in fluorescence intensity can be provided by

$$-dI/dt \cdot V \propto -V \cdot dC/dt = |J_{\text{in}} - J_{\text{out}}|$$

where  $dI/dt$  represents the change in sensor intensity,  $C$  is the concentration near the sensor, and  $V$  is the volume around the sensor. The parameter  $J_{\text{in}}$  and  $J_{\text{out}}$  are assumed constant transport rate of analyte, into and out of the chamber housing the sensor (an approximation)

$$t = V \cdot C_0 / |J_{\text{in}} - J_{\text{out}}|$$

In the first case of a 96 well-plate, the system is closed so  $J_{\text{out}} = 0$ . The timescale for the response is set by

$t_{\text{in vitro}} = V \times C_0 / J_{\text{in}}$ . Within the 96 well-plate, the approximate volume around the sensor is 250  $\mu$ L and the concentration for NO  $500 \times 10^{-6}$  M. Thus,  $t_{\text{in vitro}} = 1.25 \times 10^5 / J_{\text{in}}$ . In the second case of the leaf microfluidic chamber (Ibidi VI 0.4 slide), the dynamics of the response is influenced by both the influx and efflux rates or  $t_{\text{leaf}} = V \times C_0 / |J_{\text{in}} - J_{\text{out}}|$ . In this case, the volume of solution in the leaf chamber is approximately 50  $\mu$ L whereas the applied NO concentration is  $5000 \times 10^{-6}$  M. Thus,  $t_{\text{leaf}} = 2.5 \times 10^5 / |J_{\text{in}} - J_{\text{out}}|$ .

The  $J_{\text{in}}$  applied with the micropipette to the wells of the 96 well-plate and the leaf chamber are similar in magnitude. The  $J_{\text{out}}$  in the microfluidic channel of the leaf chamber can be calculated using Bernoulli's principle which states that the change in flow velocity between two compartments is proportional to the ratio of their cross sectional areas as  $J_{\text{out}}/J_{\text{in}} = A_{\text{in}}/A_{\text{out}}$  or  $J_{\text{out}} = J_{\text{in}} \times A_{\text{in}}/A_{\text{out}}$ . The area of the reservoir in the leaf chamber,  $A_{\text{in}}$ , is  $\times(3.8 \text{ mm})^2$  whereas the area for the microchannel  $A_{\text{out}}$  is  $3.8 \times 0.4 \text{ mm}$ . Therefore,  $J_{\text{out}} = 29.8 \times J_{\text{in}}$  and  $t_{\text{leaf}} = 8.38 \times 10^3 / J_{\text{in}}$ . From the above equations it follows that the time scale for the leaf,  $t_{\text{leaf}}$ , should be  $\approx 15$  times smaller than in vitro,  $t_{\text{in vitro}}$ . Together these results are consistent with the order of magnitude faster transients that we observe in the leaves compared to the in vitro experiments.

**Nitric Oxide Solution:** A saturated NO solution was prepared as previously described by Zhang et al.<sup>[34]</sup> Briefly, H<sub>2</sub>O (5 mL) was added to two separate 10 mL round-bottom flasks (a control and an NO sample), which were then sealed with a septum. Two needles, a gas inlet needle terminated in the liquid and an outlet needle terminated in the dead space above the liquid, were placed in the flask. Argon gas (Airgas) was bubbled into the H<sub>2</sub>O for 1 h at an outlet pressure of 2 psi to remove dissolved oxygen. The control sample was removed from the system and the needles were removed. NO gas (99.99%, Electronicfluorocarbons) was then bubbled into the NO sample for 45 min, again at an outlet pressure of 2 psi. The final NO concentration of the sample was determined using the horseradish peroxidase assay.<sup>[51,52]</sup>

## Supporting Information

Supporting Information is available from the Wiley Online Library or from the author.

## Acknowledgements

J.P.G. and M.P.L. contributed equally to this work. The authors gratefully acknowledge support from the National Science Foundation under Grant No. 1213622 (M.S.S). This material is based upon work supported by the National Science Foundation Postdoctoral Research Fellowship in Biology under Award Nos. 1103600 (J.P.G.) and 1306229 (M.P.L.), and a Burroughs Wellcome Fund under Grant No. 1013994 (M.P.L.).

[1] S. Park, M. Vosguerichian, Z. Bao, *Nanoscale* **2013**, *5*, 1727.

[2] A. M. Marconnet, N. Yamamoto, M. a Panzer, B. L. Wardle, K. E. Goodson, *ACS Nano* **2011**, *5*, 4818.

- [3] C. B. Jacobs, M. J. Peairs, B. J. Venton, *Anal. Chim. Acta* **2010**, *662*, 105.
- [4] J. Sha, T. Hasan, S. Milana, C. Bertulli, N. a W. Bell, G. Privitera, Z. Ni, Y. Chen, F. Bonaccorso, A. C. Ferrari, U. F. Keyser, Y. Y. S. Huang, *ACS Nano* **2013**, *7*, 8857.
- [5] Q. H. Wang, D. O. Bellisario, L. W. Drahushuk, R. M. Jain, S. Kruss, M. P. Landry, S. G. Mahajan, S. F. E. Shimizu, Z. W. Ulissi, M. S. Strano, *Chem. Mater.* **2014**, *26*, 172.
- [6] M. P. Landry, S. Kruss, J. T. Nelson, G. Bisker, N. M. Iverson, N. F. Reuel, M. S. Strano, *Sensors (Basel)* **2014**, *14*, 16196.
- [7] A. A. Boghossian, J. Zhang, P. W. Barone, N. F. Reuel, J.-H. Kim, D. A. Heller, J.-H. Ahn, A. J. Hilmer, A. Rwei, J. R. Arkalud, C. T. Zhang, M. S. Strano, *ChemSusChem* **2011**, *4*, 848.
- [8] J. Zhang, M. P. Landry, P. W. Barone, J.-H. Kim, S. Lin, Z. W. Ulissi, D. Lin, B. Mu, A. A. Boghossian, A. J. Hilmer, A. Rwei, A. C. Hinckley, S. Kruss, M. A. Shandell, N. Nair, S. Blake, F. Şen, S. Şen, R. G. Croy, D. Li, K. Yum, J.-H. Ahn, H. Jin, D. A. Heller, J. M. Essigmann, D. Blankschtein, M. S. Strano, *Nat. Nanotechnol.* **2013**, *8*, 959.
- [9] T. Doussineau, A. Schulz, A. Lapresta-Fernandez, A. Moro, S. Körsten, S. Trupp, G. J. Mohr, *Chemistry (Easton)*. **2010**, *16*, 10290.
- [10] B. S. Flavel, K. E. Moore, M. Pfohl, M. M. Kappes, F. Henrich, *ACS Nano* **2014**, *8*, 1817.
- [11] C. Y. Khripin, J. A. Fagan, M. Zheng, *J. Am. Chem. Soc.* **2013**, *135*, 6822.
- [12] J. G. Clar, T. Yuan, Y. Zhao, J.-C. J. Bonzongo, K. J. Ziegler, *J. Phys. Chem. C* **2014**, *118*, 15495.
- [13] K. Tvrdy, R. M. Jain, R. Han, A. J. Hilmer, T. P. McNicholas, M. S. Strano, *ACS Nano* **2013**, *7*, 1779.
- [14] R. M. Jain, K. Tvrdy, R. Han, Z. Ulissi, M. S. Strano, *ACS Nano* **2014**, *8*, 3367.
- [15] H. Liu, D. Nishide, T. Tanaka, H. Kataura, *Nat. Commun.* **2011**, *2*, 1.
- [16] P. W. Barone, S. Baik, D. A. Heller, M. S. Strano, *Nat. Mater.* **2005**, *4*, 86.
- [17] N. M. Iverson, P. W. Barone, M. Shandell, L. J. Trudel, S. Sen, F. Sen, V. Ivanov, E. Atolia, E. Farias, T. P. McNicholas, N. Reuel, N. M. a Parry, G. N. Wogan, M. S. Strano, *Nat. Nanotechnol.* **2013**, *8*, 873.
- [18] S. Kruss, M. P. Landry, E. Vander Ende, B. M. A. Lima, N. F. Reuel, J. Zhang, J. Nelson, B. Mu, A. Hilmer, M. Strano, *J. Am. Chem. Soc.* **2014**, *136*, 713.
- [19] J. P. Giraldo, M. P. Landry, S. M. Faltermeier, T. P. McNicholas, N. M. Iverson, A. A. Boghossian, R. NF, A. J. Hilmer, F. Sen, J. A. Brew, M. S. Strano, *Nat. Mater.* **2014**, *13*, 400.
- [20] D. A. Heller, H. Jin, B. M. Martinez, D. Patel, B. M. Miller, T. Yeung, P. V Jena, C. Hobartner, T. Ha, S. K. Silverman, M. S. Strano, *Nat. Nanotechnol.* **2009**, *4*, 114.
- [21] A. L. Antaris, J. T. Robinson, O. K. Yaghi, G. Hong, S. Diao, R. Luong, H. Dai, *ACS Nano* **2013**, *7*, 3644.
- [22] B. S. Flavel, K. E. Moore, M. Pfohl, M. M. Kappes, F. Henrich, *ACS Nano* **2014**, *8*, 1817.
- [23] I. S. Zulfugarov, A. Tovuu, J.-H. Kim, C.-H. Lee, *J. Plant Biol.* **2011**, *54*, 351.
- [24] I. Foissner, D. Wendehenne, C. Langebartels, J. Durner, *Plant J.* **2000**, *23*, 817.
- [25] A. Besson-Bard, A. Pugin, D. Wendehenne, *Annu. Rev. Plant Biol.* **2008**, *59*, 21.
- [26] C. H. Foyer, G. Noctor, *New Phytol.* **2000**, *146*, 359.
- [27] H. Oh, J. Sim, S.-Y. Ju, *Langmuir* **2013**, *29*, 11154.
- [28] M. Kozlov, M. Quarmyne, W. Chen, T. J. McCarthy, *Macromolecules* **2003**, *36*, 6054.
- [29] S. Dumitriu, in *Polymeric Biomaterials*, CRC Press, London **2001**, pp. 213–214.
- [30] A. Meister, A. Kerth, A. Blume, *J. Phys. Chem. B* **2004**, *108*, 8371.
- [31] C. Heitz, R. K. Prud'homme, J. Kohn, *Macromolecules* **1999**, *32*, 6658.
- [32] L. Stobiński, E. L. B. Polaczek, K. Rêbilas, J. Mazurkiewicz, R. Wrzaliak, H. Lin, P. Tomasik, *Polimery* **2008**, *7*, 571.
- [33] H. Jin, D. A. Heller, M. Kalbacova, J. H. Kim, J. Q. Zhang, A. A. Boghossian, N. Maheshri, M. S. Strano, *Nat. Nanotechnol.* **2010**, *5*, 302.
- [34] J. Zhang, A. A. Boghossian, P. W. Barone, A. Rwei, J.-H. Kim, D. Lin, D. A. Heller, A. J. Hilmer, N. Nair, N. F. Reuel, M. S. Strano, *J. Am. Chem. Soc.* **2011**, *133*, 567.
- [35] A. Pomorski, T. Kochańczyk, *Anal. Chem.* **2013**, *85*, 11479.
- [36] S. G. Rhee, T.-S. Chang, W. Jeong, D. Kang, *Mol. Cells* **2010**, *29*, 539.
- [37] E. W. Miller, C. J. Chang, *Curr. Opin. Chem. Biol.* **2007**, *11*, 620.
- [38] M. H. Lim, D. Xu, S. J. Lippard, *Nat. Chem. Biol.* **2006**, *2*, 375.
- [39] E. M. Hetrick, M. H. Schoenfish, *Annu. Rev. Anal. Chem.* **2009**, *2*, 409.
- [40] S. J. Swanson, W.-G. Choi, A. Chanoca, S. Gilroy, *Annu. Rev. Plant Biol.* **2011**, *62*, 273.
- [41] X. Zhang, W.-S. Kim, N. Hatcher, K. Potgieter, L. L. Moroz, R. Gillette, J. V Sweedler, *J. Biol. Chem.* **2002**, *277*, 48472.
- [42] S. M. Driever, M. J. Fryer, P. M. Mullineaux, N. R. Baker, in *Plant Signal Transduction* (Ed: T. Pfannschmidt), Humana Press, Totowa, NJ **2009**, pp.109–116.
- [43] J. Vitecek, V. Reinohl, R. L. Jones, *Mol. Plant* **2008**, *1*, 270.
- [44] A. Arora, R. Sairam, G. Srivastava, *Curr. Sci.* **2002**, *82*, 1227.
- [45] P. Rivera Gil, C. Vazquez-Vazquez, V. Giannini, M. P. Callao, W. J. Parak, M. A. Correa-Duarte, R. A. Alvarez-Puebla, *Angew. Chem. Int. Ed. Engl.* **2013**, *52*, 13694.
- [46] J.-H. Kim, D. A. Heller, H. Jin, P. W. Barone, C. Song, J. Zhang, L. J. Trudel, G. N. Wogan, S. R. Tannenbaum, M. S. Strano, *Nat. Chem.* **2009**, *1*, 473.
- [47] Q. L. Liu, B. Chen, Q. L. Wang, X. L. Shi, Z. Y. Xiao, J. X. Lin, X. H. Fang, *Nano Lett.* **2009**, *9*, 1007.
- [48] N. Carpita, D. Sabularse, D. Montezinos, D. P. Delmer, *Science* **2013**, *205*, 1144.
- [49] K. Yum, J.-H. Ahn, T. P. McNicholas, P. W. Barone, B. Mu, J.-H. Kim, R. M. Jain, M. S. Strano, *ACS Nano* **2012**, *6*, 819.
- [50] G. Bisker, N. M. Iverson, J. Ahn, M. S. Strano, *Adv. Healthcare Mater.* **2015**, *4*, 87.
- [51] H. Kojima, N. Nakatsubo, K. Kikuchi, S. Kawahara, Y. Kirino, H. Nagoshi, Y. Hirata, T. Nagano, *Anal. Chem.* **1998**, *70*, 2446.
- [52] K. Kikuchi, T. Nagano, M. Hirobe, *Biol. Pharm. Bull.* **1996**, *19*, 649.

Received: November 4, 2014  
 Revised: February 16, 2015  
 Published online: May 15, 2015